International Journal of Modern Physics B
Vol. 18, No. 12 (2004) 1659–1678

World Scientific
www.worldscientific.com

HOW TO READ A MOLECULAR CLOCK WITH SUB-FEMTOSECOND ACCURACY

X. M. TONG

J. R. Macdonald Laboratory, Physics Department, Kansas State University, Manhattan, Kansas 66506-2604, USA
xmtong@phys.ksu.edu

C. D. LIN

J. R. Macdonald Laboratory, Physics Department, Kansas State University, Manhattan, Kansas 66506-2604, USA and
Physics Division, National Center for Theoretical Sciences, P.O. Box 2-131, Hsinchu, 30013, Taiwan
cdlin@phys.ksu.edu

Received 20 June 2004

We analyze the elementary processes leading to the double ionization of D_2 molecules by a single femtosecond intense laser pulse. From the total kinetic energy release of the two D^+ ions which exhibits distinct peaks depending on the laser intensity, pulse length and mean wavelength, we show that the double ionization of D_2 by a short femtosecond laser pulse can serve as a molecular clock. We discuss how to read such a clock correctly and how to choose laser parameters so the clock can be read more accurately.

Keywords: Molecular clock; femtosecond laser; rescattering induced double ionization; sequential double ionization.

1. Introduction

The motion of atoms in molecules and most of chemical reactions occur on a timescale of femtoseconds and picoseconds. The general scheme to track such motion has been clear for sometime: generate a short-lived excitation of the system to initiate a reaction, and then follow the changing atomic structure of the reactant over varying time intervals. With the availability of femtosecond lasers, time resolved study of processes involving such movements have been achieved.[1] In such typical pump–probe experiments, the time resolution of the experiment is limited by the duration of the pump and/or the probe pulses. With the vibrational periods of H_2 and D_2 molecules in the range of a few tens of femtoseconds, pump–probe experiments cannot be used directly to study their dissociation or ionization dynamics. However, in a series of recent experiments,[2–4] it has been demonstrated that the time evolution of the dissociation and ionization dynamics of H_2 and D_2

can be probed with a single femtosecond pulse by measuring the kinetic energy release (KER) of the products. In such experiments, the oscillating laser electric field serves as the pump at the early cycles, while the electric field at the later cycles provides as the probe. To read the dissociation or ionization time (or the molecular clock) correctly from the measured KER, a thorough theoretical understanding of the reaction dynamics is needed. In this review, we outline the basic theoretical model for understanding these experiments and how to read the molecular clocks accurately. We will describe the double ionization of D_2 specifically, even though the theory clearly can be applied to H_2 with little modifications.

The double ionization of D_2 in an intense laser pulse is depicted schematically in Fig. 1. The D_2 molecule is ionized initially at some time t_0 when the laser electric field is near the peak. This first ionization provides the "pump" and releases an electron into the laser field. It also starts the molecular clock by sending out a nuclear vibrational wave packet. The clock stops and the time is measured when the second electron is ionized. Since the second ionization leads to two bare D^+

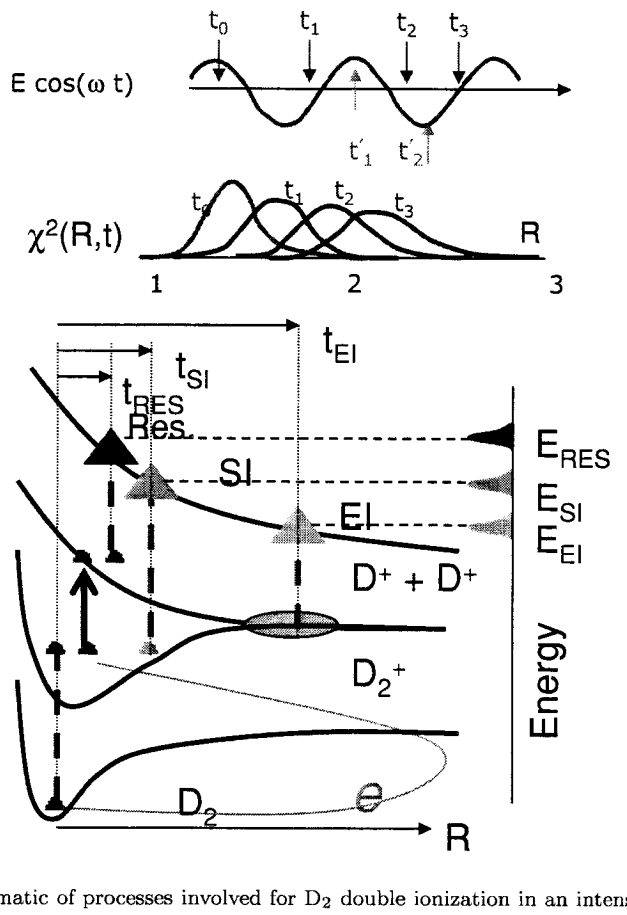

Fig. 1. Schematic of processes involved for D_2 double ionization in an intense laser field.

ions, the distance of the two
released kinetic energy of the
calculated time of propagation
the clock accurately one need
determine factors that limit th

In Fig. 1, we depict the ti
laser pulse. The D_2 molecule is
rium distance at t_0 when the el
launches a nuclear wave packe
by the ground electronic poten
anisms" where the D_2^+ ions ca

(1) the rescattering (RS) proc
(2) the sequential ionization (
(3) the charge resonance enha

In RS, the tunnelled electron i
field to excite or ionize the pare
after the laser field reaches the
is ionized at later laser cycles (
larger internuclear separations
the binding energy of D_2^+ is hi
laser intensity. For the EI, it o
lowest nearly degenerate σ_g a
laser field and tunnelling ioniza
EI is the main ionization mec
release and has been extensivel
peaks from these three ionizati

Among the three ionization
use the EI to read a molecular
the potential curves are rather
accurately deduced from the me
near the outer classical turnin
from multiple returns would me
only on ionizations where the
and SI can be used to read the
for lasers at higher intensity. S
are quite different, SI is best s
field at the early cycles of the p
later cycles where the peak field
10^{15} W/cm^2.[12] For the RS, it i
Of course RS and SI will coexis

Among the three mechanis
be measured is the first return

e by measuring the kinetic energy
ments, the oscillating laser electric
e the electric field at the later cycles
or ionization time (or the molecular
rough theoretical understanding of
w, we outline the basic theoretical
l how to read the molecular clocks
ion of D_2 specifically, even though
tle modifications.
er pulse is depicted schematically in
ome time t_0 when the laser electric
vides the "pump" and releases an
molecular clock by sending out a
ps and the time is measured when
d ionization leads to two bare D^+

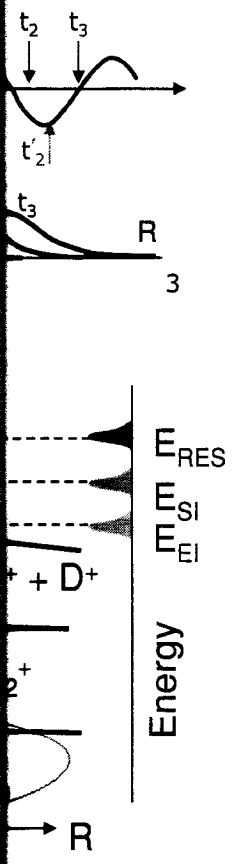

ble ionization in an intense laser field.

ions, the distance of the two nuclei at that time can be deduced from the total released kinetic energy of the two D^+ ions. The molecular clock is read from the calculated time of propagation of the nuclear wave packet to this distance. To read the clock accurately one needs to understand the double ionization dynamics to determine factors that limit the precise reading of the clock.

In Fig. 1, we depict the time-dependent electric field of a typical Ti-Sapphire laser pulse. The D_2 molecule is assumed to be ionized by tunnelling from its equilibrium distance at t_0 when the electric field is near the maximum. This first ionization launches a nuclear wave packet, where the motion of the wave packet is governed by the ground electronic potential curve of D_2^+. There are three well-known "mechanisms" where the D_2^+ ions can be further ionized:

(1) the rescattering (RS) process,
(2) the sequential ionization (SI), and
(3) the charge resonance enhanced ionization (EI).

In RS, the tunnelled electron is driven back at around t_1 (see Fig. 1) by the laser field to excite or ionize the parent ion. If it is excited the D_2^+ is ionized immediately after the laser field reaches the next maximum at t_1' or later such as t_2'. In SI, the D_2^+ is ionized at later laser cycles (such as at t_1' or t_2') when the wave packet travels to larger internuclear separations where the ionization energy becomes smaller. Since the binding energy of D_2^+ is higher than that of D_2, SI is important only at higher laser intensity. For the EI, it occurs at large internuclear distances where the two lowest nearly degenerate σ_g and σ_u potential curves are coupled strongly by the laser field and tunnelling ionization is strongly enhanced. At lower laser intensities, EI is the main ionization mechanism; it is characterized by small kinetic energy release and has been extensively studied in the past.[5–11] The typical kinetic energy peaks from these three ionization mechanisms of D_2^+ are sketched in Fig. 1.

Among the three ionization mechanisms discussed above, it is not desirable to use the EI to read a molecular clock. EI occurs at large internuclear distances where the potential curves are rather flat such that precise internuclear distance cannot be accurately deduced from the measured kinetic energy release. Furthermore, it occurs near the outer classical turning point of the nuclear wave packet and ionizations from multiple returns would mess up the clock. We can exclude EI by concentrating only on ionizations where the released kinetic energy is more energetic. Both RS and SI can be used to read the molecular clock, with SI being the main mechanism for lasers at higher intensity. Since the electric fields needed to ionize D_2 and D_2^+ are quite different, SI is best studied with short pulses where the weaker electric field at the early cycles of the pulse ionizes D_2, and the D_2^+ is further ionized at the later cycles where the peak field is substantially higher, e.g., at laser intensity above 10^{15} W/cm^2.[12] For the RS, it is best for laser intensity below 2×10^{14} W/cm^2.[2–4] Of course RS and SI will coexist at peak intensities in between.[13,14]

Among the three mechanisms, for the 800 nm laser, the shortest time that can be measured is the first return time for the RS process, which is around 1.9 fs. The

time for SI depends strongly on the pulse duration. For laser pulses of the order of 10 fs, the SI occurs at about 4.0 fs later. For EI, it occurs first at about 10 fs after the first ionization. To read the clock more accurately, i.e., to extract the molecular clock more precisely from the measured kinetic energy release spectra, the ionization dynamics has to be analyzed carefully. We will focus mostly on the RS here since it has the richest underlying physics involved. It is also the most important mechanism for producing higher D^+ kinetic energies. The SI mechanism is relatively straightforward, see Tong and Lin.[15]

In the rescattering mechanism for double ionization, one needs to calculate tunnelling ionization rates of D_2 from the ground state, the excitation cross sections of D_2^+ by the returning electron and the further ionization of D_2^+ from its excited electronic states at different internuclear distances. These electronic processes have to be folded with the time-dependent nuclear wave packet in order to extract the time information from the kinetic energy spectra of D^+ ions that are determined experimentally. The theoretical modelling is described in Section 2. Results from the theory are compared to some recent measurements in Section 3. Final remarks are given in Section 4.

2. Description of Double Ionization of D_2 by the Rescattering Mechanism

2.1. *Tunnelling ionization*

The molecular clock starts with the first ionization of D_2. While the so-called ADK[16–18] theory of tunnelling ionization for atoms has been around for many years, it has failed to describe the ionization of molecules.[19–24] Only recently has the ADK theory been extended to molecular targets.[25] This MO–ADK theory has been used to interpret the so-called ionization suppression of molecules[23] and the extension of high-order harmonic generation cutoff in molecules.[26] The MO–ADK theory also predicts the dependence of the ionization probability[27] on the alignment of the molecular axis with respect to the laser polarization. Such alignment dependence has been confirmed experimentally recently.[13,28,29] The advantage of the MO–ADK theory is that the ionization rates are expressed in analytical form — the parameters needed in the theory for each molecular orbital are only calculated once. The ionization is assumed to follow the Frank–Condon principle. Even though a recent experiment[30] demonstrated the dependence of the vibrational level distributions on the laser intensity, especially for the higher vibrational states, the vibrational wave packet is not sensitive to these variations. Following the ionization, a nuclear vibrational wave packet is created and the tunnelled electron is thrown into the laser field. The nuclear wave packet is assumed to be moving in the field of the ground electronic state potential curve of D_2^+ since the effect of the laser field on the motion of the heavy nuclei is small.

2.2. *Rescattering energy*

In the rescattering model,[31] t
changes its field direction. T
core to excite it or ionize it.
used by Yudin and Ivanov[32]
electron is treated classicall
the residual Coulomb intera
approximated by an effective
axis. To calculate the trajec
motion (Newton's second law
at $(x, y, z) = (0, 0, z_0)$, where
from the combined potential
velocity $\mathbf{v}$ is assumed to have
units $m = \hbar = e = 1$ are used

In this model, the tunnelled e
bution in velocity, i.e., we con
the transverse and longitudin
gave birth to the ionized electr
the trajectory. The distance o
for over seven optical cycles f
pulse is shorter. The distance
the time when this occurs fo
impact parameter b and the
impact (no laser field) excitat
tion starting at t_0 right after t
time the electron will revisit t
revisit the core again approxi
However, the kinetic energies
and are not important in gene
returning electron. For tunnel
field, the electron can revisit t
the figure. In the meanwhile,
at these times increases, and
mean wavelength of 800 nm.

2.3. *Electron impact excit*

For each impact parameter b
need to calculate the electron
D_2^+ at each internuclear separ
experimental or theoretical cr

2.2. *Rescattering energy spectra*

In the rescattering model,[31] the tunnelled electron will be driven back when the laser changes its field direction. The returned electron will collide with the parent ionic core to excite it or ionize it. The rescattering is modelled similar to the method used by Yudin and Ivanov[32,33] for the double ionization of helium. The ionized electron is treated classically, under the combined force from the laser field and the residual Coulomb interaction from the D_2^+ ion. For simplicity, the latter is approximated by an effective charge $Z_c = +1$ at the midpoint of the internuclear axis. To calculate the trajectory of the ionized electron, we solved the equation of motion (Newton's second law) with the initial condition that the ionized electron is at $(x, y, z) = (0, 0, z_0)$, where z_0 is the position where the electron tunnels, obtained from the combined potential of the ion and the electric field of the laser. The initial velocity $\mathbf{v}$ is assumed to have a distribution as described by the ADK model (atomic units $m = \hbar = e = 1$ are used throughout the paper unless otherwise indicated),

$$g(\mathbf{v}) \propto e^{-\mathbf{v}^2\kappa/F}. \tag{1}$$

In this model, the tunnelled electron is ejected isotropically with a Gaussian distribution in velocity, i.e., we consider the ejected electron have initial velocity in both the transverse and longitudinal directions. For each initial time t_0 or phase ϕ_0 that gave birth to the ionized electron, the classical equation of motion is solved to obtain the trajectory. The distance of the electron from the center of D_2^+ ion is monitored for over seven optical cycles for long pulses or till the end of the laser pulse if the pulse is shorter. The distance of closest approach of the electron from the ion and the time when this occurs for each trajectory are recorded. From these data, the impact parameter b and the collision energy T of the corresponding electron–ion impact (no laser field) excitation or ionization are obtained. For tunnelling ionization starting at t_0 right after the peak of the electric field of each half cycle, the first time the electron will revisit the ion core is near t_1. Without being scattered, it will revisit the core again approximately at each half optical cycle later, at $t_2, t_3, \ldots$. However, the kinetic energies of the returned electron at t_2, $t_4, \ldots$ are much smaller, and are not important in general. Figure 2 shows the typical energy spectra of the returning electron. For tunnelling ionization occurred before the peak of the laser field, the electron can revisit the core only near t_3, and they are indicated as t_3^- in the figure. In the meanwhile, the average internuclear separation of D_2^+ (and H_2^+) at these times increases, and they are tabulated in Table 1 for laser pulses with mean wavelength of 800 nm.

2.3. *Electron impact excitation and ionization*

For each impact parameter b and kinetic energy T of the returning electron, we need to calculate the electron impact excitation and ionization cross sections of D_2^+ at each internuclear separation R. Different from the He^+ case, there are few experimental or theoretical cross section data available for D_2^+. Thus we have to

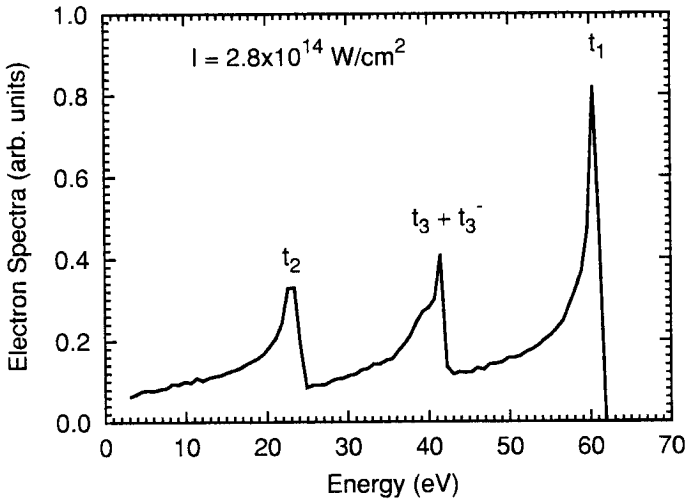

Fig. 2. Energy spectra of rescattering electron when it returns to collide with the parent ionic core.

Table 1. Relation between the returning time and the average nuclear separation for H_2^+ and D_2^+.

return	time (fs)	$\langle R \rangle$ (a.u.)	
		H_2^+	D_2^+
t_1	1.9	1.8	1.6
t_3	4.3	2.5	2.1
t_5	7.0	3.0	2.6
t_7	9.6	3.2	3.0

generate the cross sections needed semi-empirically. For each total cross section $\sigma(T)$ at kinetic energy T, we assume that the probability for excitation or ionization at impact parameter b is given by

$$P_m(b,T) = \sigma(T)\frac{e^{-b^2/a_o^2}}{\pi a_o^2}, \tag{2}$$

$$a_o = \sqrt{2/\Delta E}, \tag{3}$$

where $T = v^2/2$ and ΔE is the excitation or ionization energy. Here, the b-dependence is taken to have the Gaussian form. For the rescattering in helium, Yudin and Ivanov[32] have checked different forms of b-dependence and concluded that the results are rather insensitive to the precise functional form used.

For electron impact ionization cross section, we employ the empirical formula

$$\sigma_i(T,\Delta E) = \frac{\pi}{\Delta E^2} e^{1.5*(\Delta E-0.5)/T} f(T/\Delta E) \tag{4}$$

$$f(x) =$$

where ΔE is the ionization e
impact ionization cross sectio
intermediate energy region, re
oretical H(1s) ionization cross
0.225. The empirical formula,

(i) the ionization cross sect
internuclear separation;[3
(ii) the ionization cross sec
internuclear separation;[3
(iii) the ionization cross sec
agreement with the reco

If these are all satisfied, Eq. (
tions.

For the excitation proces
dominant channels populated
state since they have the lowe
a semi-empirical fitting proc
that the excitation cross secti
as in ionization, except that
in Eq (4) should be replaced
in atomic hydrogen. From the
Bray,[34] we obtained

$$A = 0.7638,$$

The formula was further teste
with the calculated one for

$$e^- +$$

From the total 1s → 2p excit
tion cross section to $2p_0$ or 2
as the quantization axis. The
theoretically, or deduced exp
ments. (Note: $2p_{-1}$ cross secti
fit the $2p_0$ to $2p_1$ cross sectio

$$r(x) =$$

where $x = T/\Delta E$ is the scale
much from the calculated rati

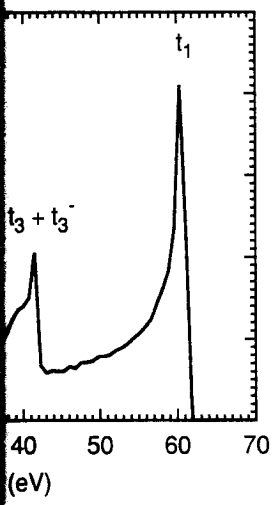

it returns to collide with the parent ionic

e returning time
tion for H_2^+ and

⟨R⟩ (a.u.)	
H_2^+	D_2^+
1.8	1.6
2.5	2.1
3.0	2.6
3.2	3.0

lly. For each total cross section $\sigma(T)$
bility for excitation or ionization at

$$\frac{-b^2/a_o^2}{\pi a_o^2}\,, \tag{2}$$

$$\overline{E}\,, \tag{3}$$

or ionization energy. Here, the b-
m. For the rescattering in helium,
ms of b-dependence and concluded
ecise functional form used.
, we employ the empirical formula

$$^{5)/T} f(T/\Delta E) \tag{4}$$

$$f(x) = \left(A \ln x + B\left(1 - \frac{1}{x}\right) - C\frac{\ln x}{x}\right)\frac{1}{x} \tag{5}$$

where ΔE is the ionization energy. The three terms in Eq. (5) represent electron impact ionization cross section in the high-energy limit, the low energy limit and the intermediate energy region, respectively. By fitting this formula to the accurate theoretical H(1s) ionization cross section[34] we obtained $A = 0.7213, B = -0,302, C = 0.225$. The empirical formula, Eq. (4), is used to make sure that:

(i) the ionization cross section is in good agreement with that of He^+ for small internuclear separation;[34]
(ii) the ionization cross section is in good agreement with that of H for large internuclear separation;[34] and
(iii) the ionization cross section of D_2^+ at equilibrium distance is in reasonable agreement with the recommended value from NIST.[35]

If these are all satisfied, Eq. (4) is expected to be valid for any internuclear separations.

For the excitation process, it is clear that the σ_u and π_u states will be the dominant channels populated via electron impact excitation from the ground σ_g state since they have the lowest excitation energies. Once more, we need to employ a semi-empirical fitting procedure for such excitation cross sections. We assume that the excitation cross section again can be fitted in the form of Eqs. (4) and (5) as in ionization, except that ΔE now is the excitation energy and the number 0.5 in Eq (4) should be replaced by the excitation energy of the corresponding state in atomic hydrogen. From the tabulated H(1s)→ H(2p) excitation cross section by Bray,[34] we obtained

$$A = 0.7638\,, \qquad B = -1,1759\,, \qquad C = -0.6706\,.$$

The formula was further tested by comparing the predicted excitation cross section with the calculated one for

$$e^- + He^+(1s) \rightarrow e^- + He^+(2p)\,.$$

From the total 1s → 2p excitation cross section, we can further distinguish excitation cross section to $2p_0$ or $2p_1$, with the direction of the incident electron beam as the quantization axis. The relative $2p_0$ and $2p_1$ cross sections can be calculated theoretically, or deduced experimentally from polarization or correlation measurements. (Note: $2p_{-1}$ cross section is identical to $2p_1$ cross section by symmetry.) We fit the $2p_0$ to $2p_1$ cross section ratio by

$$r(x) = \frac{\sigma_0}{\sigma_1} = \frac{8.2\sqrt{1 + 1.1/x^2}}{x} + 0.44 \tag{6}$$

where $x = T/\Delta E$ is the scaled kinetic energy. Since the ratio for He does not differ much from the calculated ratio for H, this comparison convinces us to use the $r(x)$

in Eq. (6) to describe the ratio for D_2^+ as well. The $r(x)$ indicates that $m = 0$ is the dominant magnetic component in the present interested energy regime.

To relate the $2p_0$ or $2p_1$ partial cross sections to the excitation cross sections of σ_u and π_u electronic states of D_2^+, we need to know the alignment angle of the molecule. If the molecule is aligned along the laser field polarization direction (which is also the direction of the electron beam), the $2p_0$ cross section is the excitation to the σ_u state and the $2p_1$ ($2p_{-1}$) cross section is for the excitation to the π_u state. If the molecule is aligned perpendicular to the laser polarization direction, then the role is reversed, i.e., $2p_1$ (or $2p_{-1}$) corresponds to the cross section of the σ_u excitation, and $2p_0$ cross section to the π_u excitation. For any arbitrary alignment angle θ of D_2^+, we assume that the total excitation cross sections to σ_u and π_u are given by

$$\sigma(\sigma_u) = \sigma_T(r_0 \cos^2\theta + r_1 \sin^2\theta)\,, \tag{7}$$

$$\sigma(\pi_u) = \sigma_T(r_0 \sin^2\theta + r_1 \cos^2\theta)\,, \tag{8}$$

$$\sigma_T = \sigma_0 + 2\sigma_1\,, \tag{9}$$

$$r_0 = \frac{\sigma_0}{\sigma_T} = \frac{r(x)}{r(x)+2}\,, \tag{10}$$

$$r_1 = \frac{2\sigma_1}{\sigma_T} = \frac{2}{r(x)+2}\,. \tag{11}$$

The semi-empirically fitted electron impact ionization or excitation cross section formulae discussed so far are for a free electron colliding with an atomic or molecular ion. For the rescattering process, the two electrons in D_2 initially are in the singlet state ($S = 0$). Thus in principle, one should just use singlet excitation or ionization cross sections, instead of the spin-averaged cross sections. We obtain the singlet cross sections from the total cross section following the empirical formula derived in Yudin and Ivanov[33] [their Eqs. (8) and (9)].

These empirical formulae allow us to calculate electron impact excitation cross sections from σ_g to σ_u and to π_u at each internuclear separation and at each alignment angle of the D_2^+ ion. We obtained the ratio of the cross section of σ_u with respect to π_u, and compared the result with the ratio obtained by Peek[36] where the impact excitation cross sections for different internuclear separations were calculated using the Born approximation. The agreement is quite good, with the average cross section for σ_u about a factor of two larger than for π_u. The absolute cross sections from Peek are larger since Born approximation was used.

We also consider the small contribution from excitation to the $2s\sigma_g$ electronic state of D_2^+. The empirical formula is chosen to be

$$\sigma_e(T, \Delta E) = \frac{1}{\Delta E^2} f(T/\Delta E)\,, \tag{12}$$

$$f(x) = \frac{1}{x}\frac{A}{1 + B/x}\,, \tag{13}$$

where the parameters $A = 0$
the 1s → 2s excitation cross
independent of the alignment

2.4. *Impact excitation pr*

With all the elementary cross
ity distribution of exciting D_2^+
state σ_g to a specific excited e
tron where the returning elec
the laser over one-half optical

$$\frac{dP_m}{dR} = \frac{\int\int P_m(}{}$$

The subscript m stands for th
the impact excitation or ioniz
is the MO–ADK rate for ioniz
field strength of the laser. Fo
with an initial velocity $\mathbf{v}$, with
both the longitudinal and tra
initial velocity and position
distance of closest approach,
kinetic energy T are calculat
At each return time t_r, the d
is used to calculate the prob
In this expression the MO–A
the σ_u and π_u states depend
are isotropic. For D_2 initially
polarization of the laser, the
one-half optical cycle are sho
($I_0 = 10^{14}$ W/cm^2). Note tha
that to σ_u is also significant.

From the simulation, we c
tion spectra from each individ
in Fig. 3 show that direct im
small. The rescattering mostl
dissociation of D_2^+ from an e
energy given by

shared equally by D and D^+.
rescattering process peaks at
acteristic rescattering time t_r
gies probes directly the recoll

The $r(x)$ indicates that $m = 0$ is the
interested energy regime.
ions to the excitation cross sections
to know the alignment angle of the
er field polarization direction (which
$2p_0$ cross section is the excitation to
is for the excitation to the π_u state.
e laser polarization direction, then
onds to the cross section of the σ_u
itation. For any arbitrary alignment
tion cross sections to σ_u and π_u are

$$+ r_1 \sin^2\theta)\,, \tag{7}$$

$$+ r_1 \cos^2\theta)\,, \tag{8}$$

$$\tag{9}$$

$$\overline{2}\,, \tag{10}$$

$$\overline{+2}\,. \tag{11}$$

onization or excitation cross section
colliding with an atomic or molecular
rons in D_2 initially are in the singlet
t use singlet excitation or ionization
oss sections. We obtain the singlet
owing the empirical formula derived

late electron impact excitation cross
nuclear separation and at each align-
atio of the cross section of σ_u with
the ratio obtained by Peek[36] where
internuclear separations were calcu-
ment is quite good, with the average
ger than for π_u. The absolute cross
ximation was used.
om excitation to the $2s\sigma_g$ electronic
o be

$$(T/\Delta E)\,, \tag{12}$$

$$\frac{A}{\sqrt{B/x}}\,, \tag{13}$$

where the parameters $A = 0.17, B = 1.53$ are obtained by fitting the formula to the $1s \rightarrow 2s$ excitation cross sections of H. This cross section is assumed to be independent of the alignment of the molecular ion.

2.4. *Impact excitation probability by the tunnelled electron*

With all the elementary cross sections available, we can now calculate the probability distribution of exciting D_2^+ at a given internuclear separation R from the ground state σ_g to a specific excited electronic state or ionized states by the returning electron where the returning electron originates from the ionization of D_2 molecule by the laser over one-half optical cycle. The probability distribution is calculated from

$$\frac{dP_m}{dR} = \frac{\int\int P_m(b,T)\chi^2(R,t_r)g(\mathbf{v})W(F\cos\phi)d\mathbf{v}d\phi}{\int\int g(\mathbf{v})W(F\cos\phi)d\mathbf{v}d\phi}\,. \tag{14}$$

The subscript m stands for the excited states ($\sigma_u, \pi_u, \sigma_g$) or ionization. $P_m(b,T)$ is the impact excitation or ionization probability from Eq. (2). In this expression, W is the MO–ADK rate for ionizing D_2 at the static field $F\cos\phi$, where F is the peak field strength of the laser. For each ϕ, the tunnelled electron leaves the molecule with an initial velocity $\mathbf{v}$, with a distribution governed by Eq. (1), i.e., effects due to both the longitudinal and transverse velocity distributions are included. For each initial velocity and position of the tunnelled electron, the return time t_r at the distance of closest approach, the corresponding laser-free impact parameter b and kinetic energy T are calculated, and the excitation probability is also calculated. At each return time t_r, the distribution of the vibrational wave packet, $\chi^2(R,t_r)$, is used to calculate the probability of finding D_2^+ at internuclear separation R. In this expression the MO–ADK rates and the impact excitation probabilities to the σ_u and π_u states depend on the alignment of molecules. The other quantities are isotropic. For D_2 initially aligned perpendicular to the direction of the linear polarization of the laser, the impact excitation probabilities at different R's over one-half optical cycle are shown in Fig. 3, where the peak laser intensity is $2.8\ I_0$ ($I_0 = 10^{14}$ W/cm^2). Note that the excitation probability to π_u is the largest, but that to σ_u is also significant.

From the simulation, we can also decompose the impact excitation and ionization spectra from each individual return. For peak laser intensity of $2.8\ I_0$ the results in Fig. 3 show that direct impact ionization of D_2^+ by the rescattering electron is small. The rescattering mostly populates D_2^+ in the excited π_u and σ_u states. The dissociation of D_2^+ from an excited electronic state would release a total kinetic energy given by

$$U(R_0) - U(\infty)\,,$$

shared equally by D and D^+, respectively. According to Fig. 3, excitation by the rescattering process peaks at characteristic internuclear separations related to characteristic rescattering time t_r, thus measurement of the D^+ fragment kinetic energies probes directly the recollision times. This forms the basis of molecular clocks

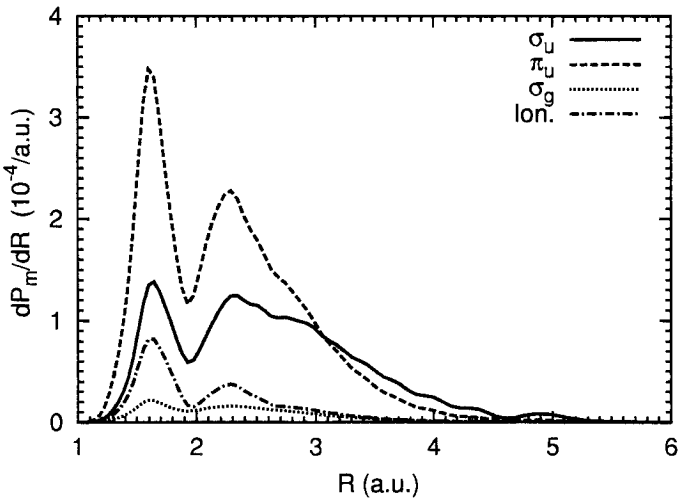

Fig. 3. Electron impact excitation and ionization probabilities of D_2^+ by the rescattering electron following tunnelling ionization of D_2 by a short pulse laser with peak intensity of 2.8 I_0 ($I_0 = 10^{14}$ W/cm^2) and pulse length of 30 fs.

in the experiments of Niikura *et al.*[2,3] However, as shown in Tong *et al.*[37,38] and in Alnaser *et al.*,[4] the excited D_2^+ ions are still in the laser field and they can be further ionized by the lasers. Thus we need to calculate the fractions of the further ionization by the laser field and the kinetic energy spectra of D^+ resulting from the subsequent Coulomb explosion.

2.5. *Field ionization of the excited D_2^+ ion*

In this subsection we consider the ionization of D_2^+ from the excited electronic states. We emphasize that we will consider peak laser intensity within $0.5 \sim 5$ I_0 only where rescattering is important. In this intensity region, D_2^+ is readily ionized if it is in the π_u excited state since its saturation intensity is only about 0.1 I_0 because of its small ionization energy. Thus we need only to calculate the ionization rate of D_2^+ from the σ_u state. If the initial excitation to σ_u occurs at R, the total accumulated probability for ionizing an electron by the laser field from the σ_u state is

$$P_i(R,\infty) = 1 - e^{-\int W(R')dt} = 1 - e^{-\int_R^\infty W(R')/v(R')dR'}, \quad (15)$$

with $$\frac{1}{2}\mu v^2(R') = U(R) - U(R'). \quad (16)$$

where $W(R')$ is the MO–ADK tunnelling ionization rate described in Section 2.1, μ is the reduced mass of the two nuclei, and $U(R)$ is the total potential energy of

the σ_u state. The σ_u state cre
release a kinetic energy

$$E_i(R$$

Here we are more interested i
by

$$\frac{dP_i(R,R')}{dR'} =$$

or in terms of differential pro

$$\frac{dP_i}{}$$

To obtain the total ioniza
initial ionization at all values

$$\frac{dP_{\rm ion}}{dE}$$

This integration is important
For other excited electronic s
complete within one cycle o
ionization spectra for these e

The total ionization spectra a
excited electronic states, and
(very negligible).

For the dissociation proce

$$\frac{dP_{\rm dis}}{dE}$$

The total dissociation spectra
the excited electronic states.
state only. In all other excited
by the laser within one optica

3. Results and Discussion

As discussed above, the break

(1) dissociation into $D^+ + D$
(2) double ionization into D^+

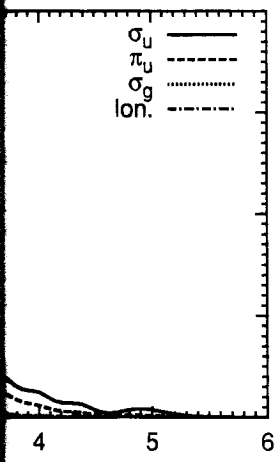

.)

abilities of D_2^+ by the rescattering electron
laser with peak intensity of 2.8 I_0 (I_0 =

er, as shown in Tong *et al.*[37,38] and
ll in the laser field and they can be
calculate the fractions of the further
rgy spectra of D^+ resulting from the

ion

of D_2^+ from the excited electronic
ak laser intensity within $0.5 \sim 5$ I_0
tensity region, D_2^+ is readily ionized
ation intensity is only about 0.1 I_0
need only to calculate the ionization
itation to σ_u occurs at R, the total
n by the laser field from the σ_u state

$V(R')dt$

$W(R')/v(R')dR'}$, (15)

$V(R')$. (16)

zation rate described in Section 2.1,
$V(R)$ is the total potential energy of

the σ_u state. The σ_u state created at R, followed by laser field ionization at R' will release a kinetic energy

$$E_i(R') = U(R) - U(R') + 1/R' .$$

Here we are more interested in the differential ionization probability which is given by

$$\frac{dP_i(R,R')}{dR'} = \frac{W(R')}{v(R')} e^{-\int_R^{R'} W(R'')/v(R'')dR''} , \tag{17}$$

or in terms of differential probability per units of kinetic energy

$$\frac{dP_i(R,R')}{dE} = \frac{dP_i(R,R')}{dR'}\frac{dR'}{dU} , \tag{18}$$

$$\frac{dR'}{dU} = \frac{1}{|\frac{dU(R')}{dR'}|} . \tag{19}$$

To obtain the total ionization spectra, we need to add up contributions from initial ionization at all values of R, i.e.,

$$\frac{dP_{\text{ion}}}{dE} = \int \frac{dP_m}{dR}\frac{dP_i(R,R')}{dE} dR . \tag{20}$$

This integration is important primarily only for ionization from the excited σ_u state. For other excited electronic states, due to their high ionization rates, ionization is complete within one cycle or less and we can set $R = R'$, and the differential ionization spectra for these excited electronic states are given by

$$\frac{dP_{\text{ion}}}{dE} = \frac{dP_m}{dR}\frac{dR}{dU} . \tag{21}$$

The total ionization spectra are obtained by adding up contributions from all the excited electronic states, and from the initial ionization by the rescattering electron (very negligible).

For the dissociation process, the energy spectra are obtained from

$$\frac{dP_{\text{dis}}}{dE} = (1 - P_i(R))\frac{dP_m}{dR}\frac{dR}{dU} . \tag{22}$$

The total dissociation spectra are calculated by adding up contributions from all the excited electronic states. In reality, the dissociation comes from the σ_u excited state only. In all other excited electronic states the D_2^+ ions are immediately ionized by the laser within one optical cycle.

3. Results and Discussion

As discussed above, the breakup of D_2 molecules in the laser field results in:

(1) dissociation into $D^+ + D$;
(2) double ionization into $D^+ + D^+$.

At lower laser intensity, double ionization comes primarily from the rescattering mechanism considered here. At higher intensity, contributions from sequential double ionization has to be included. In the following, we will compare the calculated kinetic energy release using the theoretical model presented in the previous section to compare with data from non-coincidence experiments and from coincidence experiments. From the theoretical calculations we further make predictions of the kinetic energy release spectra on the laser intensity, mean wavelength and pulse durations, to draw conditions where the molecular clock can be read with higher accuracy.

3.1. *Non-coincidence KER spectra — dissociation or ionization?*

In the experiments of Niikura *et al.*,[2] the kinetic energies of D^+ ions were measured in the direction perpendicular to the direction of laser polarization. The measured non-coincidence D^+ signals come from ionization as well as from dissociation. Thus, the measured signal can be expressed as

$$\text{Signal} \propto 2\frac{dP_{\text{ion}}}{dE} + \frac{dP_{\text{dis}}}{dE}. \tag{23}$$

Figure 4 shows the experimental D^+ kinetic energy spectra from Niikura *et al.*[2] Here the data were presented against the total breakup energy, or twice the energy of the D^+ ions, and the theoretical yield is normalized to the peak experimental value at 12 eV. The experiment was performed for a pulse of 40 fs and peak intensity of 1.5 I_0. There is a general overall agreement except the theoretical yield appears to be somewhat higher near 16 eV and the theory is lower between 5–10 eV. However it appears that the discrepancy can be reconciled if one takes into account of the volume effect in that the experimental spectra have to be integrated over a volume where the intensities are less than the peak value. The energy resolution and the finite acceptance angles can all contribute to the smoother experimental spectra. One of course should also take this "better agreement" with caution in view that the peak intensity of the laser is often not known precisely.

One of the major goals of the simulation is to unravel the origin of the structure in the kinetic energy spectra which would give insight on how the molecular clock works. For this purpose, in Fig. 5 contributions from dissociation versus ionization, and for rescattering occurred after one or two optical cycles, or equivalently, for time near the first (t_1) or the third returns (t_3), are separately displayed. From this figure we notice:

(1) ionization is much stronger than dissociation;
(2) the peak from the third return (2nd cycle) is higher than from the first return;
(3) the width of the peak from the first return is broader than the peak from the third return.

Another interesting observation is that the peak position of the dissociation spectra from the first return almost coincides with the peak position in the ionization

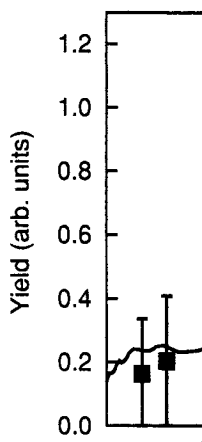

Fig. 4. D^+ energy spectra due t
intensity is 1.5 I_0 with a 40 fs puls

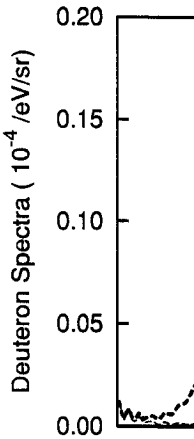

Fig. 5. Decomposition of D^+ ion
for rescattering occurring within t
ionization. The peak laser intensity

spectra from the third return.
electronic states.

In the experiment of Niik
dissociation of D_2^+ via the σ_u

omes primarily from the rescattering
y, contributions from sequential dou-
ving, we will compare the calculated
odel presented in the previous sec-
ce experiments and from coincidence
s we further make predictions of the
tensity, mean wavelength and pulse
cular clock can be read with higher

issociation or ionization?

ic energies of D^+ ions were measured
of laser polarization. The measured
on as well as from dissociation. Thus,

$$\frac{dP_{\rm dis}}{dE}. \qquad (23)$$

rgy spectra from Niikura *et al.*[2] Here
akup energy, or twice the energy of
lized to the peak experimental value
pulse of 40 fs and peak intensity of
cept the theoretical yield appears to
is lower between 5–10 eV. However
iled if one takes into account of the
have to be integrated over a volume
alue. The energy resolution and the
the smoother experimental spectra.
reement" with caution in view that
wn precisely.
to unravel the origin of the structure
insight on how the molecular clock
from dissociation versus ionization,
o optical cycles, or equivalently, for
, are separately displayed. From this

ion;
is higher than from the first return;
is broader than the peak from the

k position of the dissociation spectra
he peak position in the ionization

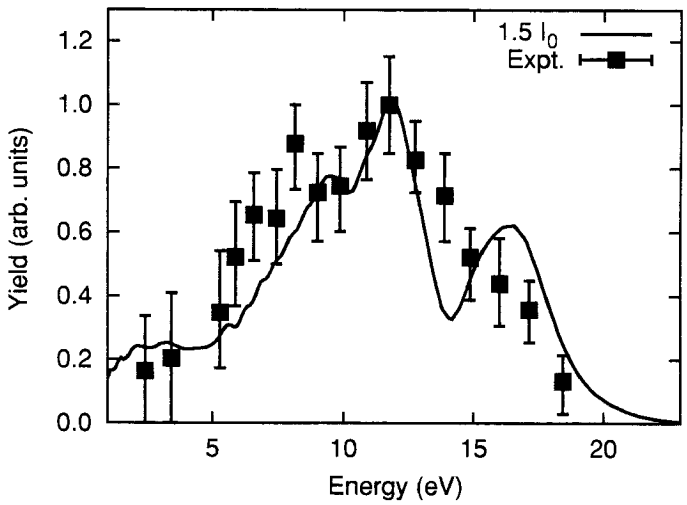

Fig. 4. D^+ energy spectra due to the breakup of D_2 in the intense laser field. The peak laser intensity is 1.5 I_0 with a 40 fs pulse duration. The experimental data are from Niikura *et al.*[2]

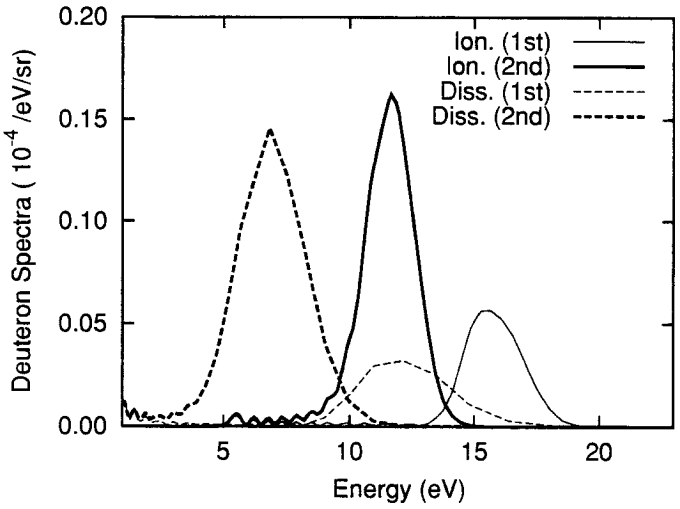

Fig. 5. Decomposition of D^+ ion yields into contributions from dissociation and ionization, and for rescattering occurring within the first and the second optical cycle after the initial tunnelling ionization. The peak laser intensity is $I = 1.5\ I_0$, and pulse length is 40 fs.

spectra from the third return. This shift is due to the binding energy of the excited electronic states.

In the experiment of Niikura *et al.*[2] the peak at 12 eV was attributed to the dissociation of D_2^+ via the σ_u curve at the first return. In other words, this peak

reads the clock at t_1. According to our simulation, the peak comes from ionization following rescattering at the third return, and this peak should read the clock at t_3. Contributions to the total D^+ signal from dissociation do become more important at lower laser intensity.[37] Even for laser intensity as low as 0.9 I_0 the peak at 12 eV still comes mostly from the ionization following rescattering at t_3. We remark that the spectra in Fig. 4 were calculated including contributions up to seven optical cycles after the initial tunnelling ionization and convergence of the calculation had been checked.

3.2. *Coincidence KER spectra*

The D^+ ion kinetic energy distributions in laser-D_2 interactions have been determined in coincidence measurements where the two D^+ ions were detected simultaneously by Staudte *et al.*[39] and more recently by Alnaser *et al.*[4] In the latter experiment, the branching ratios of ionization with respect to dissociation had been measured as well, for peak laser intensities of $1 \sim 5$ I_0. It has been found[15] that for laser intensity higher than 4 I_0, sequential double ionization process has to be taken into account. Thus the comparison in Fig. 6 is carried out for laser intensity at 2.8 I_0. The experiment used a 35 fs pulse with mean wavelength of 800 nm. The D^+ spectra are from Coulomb explosion of ions at 60–80° with respect to the laser polarization. In the figure the theoretical simulations were for laser intensity of 2.0 and 1.0 I_0, respectively. Best overall agreement with the experimental data at 2.0 I_0 was found without considering the volume effect. Note that the theoretical calculation was carried out for molecules aligned perpendicular to the laser polarization

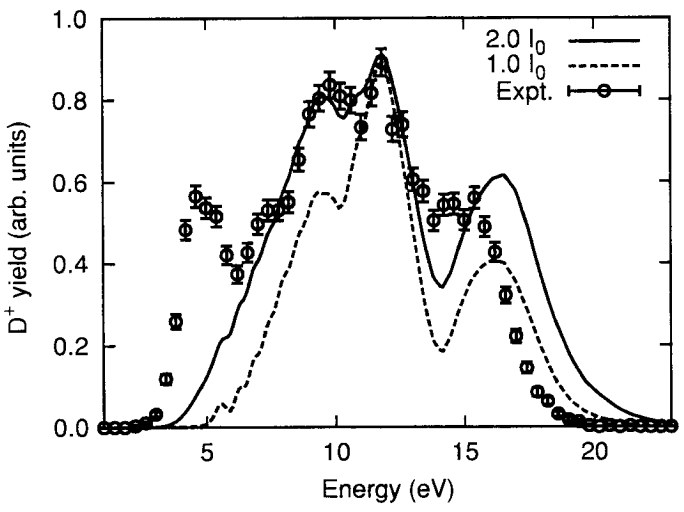

Fig. 6. Comparison of D^+ ion spectra resulting from double ionization of D_2 molecules in the intense laser field. The experiment data are from Alnaser *et al.*[4] for peak laser intensity of 2.8 I_0 and the theoretical simulation is for laser peak intensities of 2.0 and 1.0 I_0, and 35 fs pulse length.

while the experiments measu
polarization. The simulated s
agree quite well with the data
simulation. The discrepancy
to the weaker laser intensity a
energy peak is reduced signif

3.3. *Optimal laser param molecular clocks*

Based on the rescattering me
curacy in reading the molecu
strongly on the laser field int
femtoseconds, the spreading c
one excited electronic states
sections on internuclear separ
precise reading of the clock.

First consider the laser i
the energies of the rescatterin
the electron energy at the fi
the corresponding internuclea
to double ionization and one
despite that the electron has
possible since the nuclear wa
where the excitation energy is
energy spectra for 30 fs puls
intensity of 0.9 I_0 the peak fro
the peak from the first retur
et al.[39] As the intensity incr
returns can become large, ov

Next we consider the pul
nate later returns of the resc
the ultra-short pulses have be
atoms.[40] Now we apply the
the kinetic energy release spe
15 and 30 fs. For the shortest
pulse we can see major cont
the later returns show as a kn
the 5th return shows a recog
in experiments recently.[14]

Another feature that can
By increasing the mean wa

tion, the peak comes from ionization
this peak should read the clock at t_3.
sociation do become more important
ty as low as 0.9 I_0 the peak at 12 eV
g rescattering at t_3. We remark that
ng contributions up to seven optical
d convergence of the calculation had

laser-D_2 interactions have been de-
the two D^+ ions were detected si-
ently by Alnaser *et al.*[4] In the latter
with respect to dissociation had been
1 $\sim$ 5 I_0. It has been found[15] that
double ionization process has to be
ig. 6 is carried out for laser intensity
ith mean wavelength of 800 nm. The
s at 60–80° with respect to the laser
lations were for laser intensity of 2.0
t with the experimental data at 2.0
ffect. Note that the theoretical calcu-
rpendicular to the laser polarization

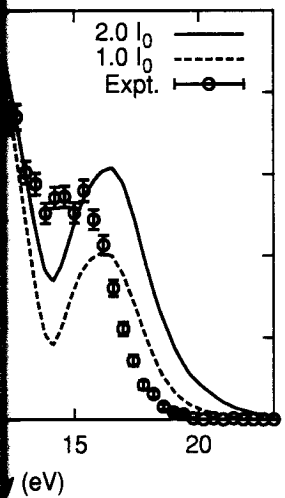

n double ionization of D_2 molecules in the
ser *et al.*[4] for peak laser intensity of 2.8 I_0
ies of 2.0 and 1.0 I_0, and 35 fs pulse length.

while the experiments measured ions leaving at 60–80° with respect to the laser polarization. The simulated spectra near the kinetic energy peak region of 7–12 eV agree quite well with the data, but the peak near 17 eV is more pronounced in the simulation. The discrepancy probably can be attributed to the volume effect. Due to the weaker laser intensity away from the focal point, its contribution to the high energy peak is reduced significantly, as shown in Fig. 6 for 1.0 I_0.

3.3. *Optimal laser parameters for accurately reading molecular clocks*

Based on the rescattering mechanism we now discuss factors that control the accuracy in reading the molecular clock. While tunnelling ionization which depends strongly on the laser field intensity confines the duration of each ionization to subfemtoseconds, the spreading of the nuclear wave packet, the excitation of more than one excited electronic states of D_2^+ and the dependence of impact excitation cross sections on internuclear separations by the returning electron all tend to limit the precise reading of the clock.

First consider the laser intensity. When we tune the laser intensity, we tune the energies of the rescattering electron (as shown in Fig. 2). At lower intensity, if the electron energy at the first return t_1 is smaller than the excitation energy at the corresponding internuclear distance, then the first return does not contribute to double ionization and one has to wait for later returns. At the third return t_3, despite that the electron has smaller energy, excitation by the returning electron is possible since the nuclear wave packet has moved to a larger internuclear distance where the excitation energy is smaller. In Fig. 7 we show the calculated total kinetic energy spectra for 30 fs pulses at three different intensities. Clearly at the lower intensity of 0.9 I_0 the peak from the third return is relatively more pronounced than the peak from the first return. This is consistent with the observation of Staudte *et al.*[39] As the intensity increases such as at 2.7 I_0, contributions from the later returns can become large, overtaking the 3rd return peak.

Next we consider the pulse duration dependence. A short pulse would eliminate later returns of the rescattering electron. Elimination of the later returns in the ultra-short pulses have been observed in non-sequential double ionization from atoms.[40] Now we apply the idea to select a particular return. In Fig. 8 we show the kinetic energy release spectra from the double ionization of D_2 by pulses of 8, 15 and 30 fs. For the shortest pulse only the first return contributes. For the 15 fs pulse we can see major contributions from the third and the first returns, while the later returns show as a knee in the low energy region. For the 30 fs pulse, even the 5th return shows a recognizable peak. These predictions have been confirmed in experiments recently.[14]

Another feature that can be varied is the mean wavelength of the laser pulse. By increasing the mean wavelength the period of each optical cycle increases

correspondingly and the time for each return also increases proportionally. Thus by going to longer wavelength, the kinetic energy release will shift to the lower energy. Figure 9 showed the calculated kinetic energy distribution for an 8 fs pulse with peak intensity of 1.5 I_0 at three wavelengths. The single peak for each wavelength comes from the first return, and its position shifts to lower energy as the wavelength is increased.

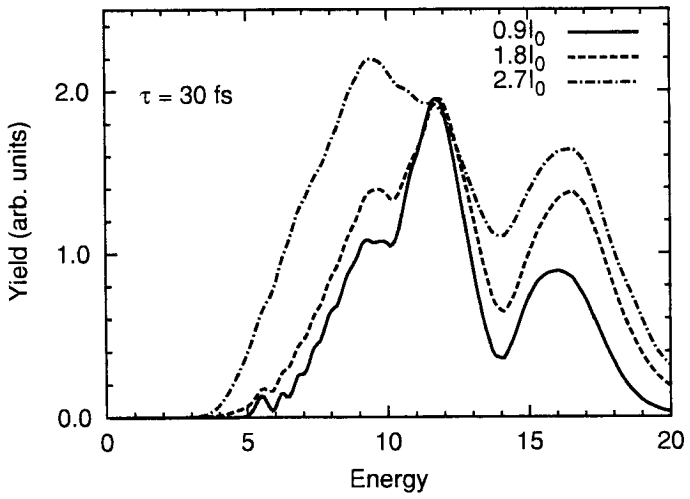

Fig. 7. D_2 total kinetic energy release spectra for several laser intensities with 30 fs pulse duration. The spectra are normalized at the peak from the third return.

Fig. 8. D_2 total kinetic energy release spectra for several laser intensities with different pulse durations. All the spectra are normalized at the 1st return peak.

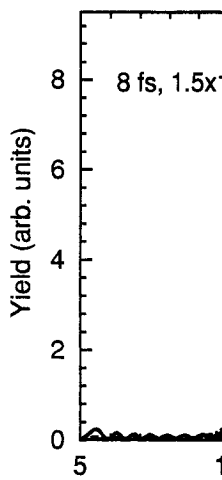

Fig. 9. D_2 total kinetic energy rel
intensity of 1.5 I_0 and pulse durac

3.4. *Sequential double ion laser field*

A molecular clock can be "buil
if it is a short pulse. The mec
sequential double ionization.
simpler, and has been descrit
the early cycles of the pulse.
and the peak power is reache
shorter pulse would take fewe
the D_2^+ can be ionized. Figure
peak intensity of 3.0×10^{15} W/
peak of the kinetic energy rel
as the pulse length is increase
of the second ionization with
interval after the first ionizat
about 2.6 fs after the first ion
pulse, it is about 4 fs, or three
full optical cycles later. In ot
in Fig. 10 as reading of the
right to left. From the width
with sub-femtosecond accurac
laser pulses has been studied
been investigated experimenta

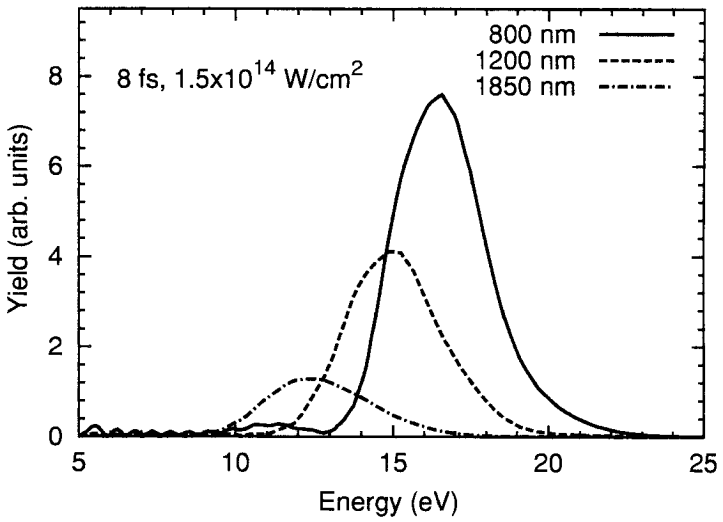

Fig. 9. D_2 total kinetic energy release spectra for different mean wavelengths but at a fixed laser intensity of 1.5 I_0 and pulse duraction of 8 fs.

3.4. *Sequential double ionization in a super-intense short pulse laser field*

A molecular clock can be "built" based on double ionization of D_2 at high intensities if it is a short pulse. The mechanism for double ionization at high intensities is the sequential double ionization. The basic physics of sequential double ionization is simpler, and has been described elsewhere.[15] The first ionization of D_2 occurs at the early cycles of the pulse. For a short pulse, the electric field increases rapidly and the peak power is reached in a few half cycles. For a given peak intensity, a shorter pulse would take fewer half-cycles for the pulse to reach the intensity that the D_2^+ can be ionized. Figure 10 shows the kinetic energy release of the D^+ ions at peak intensity of 3.0×10^{15} W/cm^2 and pulse lengths of 4, 7 and 14 fs. Note that the peak of the kinetic energy release shifts from 15 eV to 13 eV and then to 10.5 eV as the pulse length is increased. Figure 11 is a plot showing the probability density of the second ionization with respect to the internuclear separation and the time interval after the first ionization. For the 4 fs pulse, the 2nd ionization occurs at about 2.6 fs after the first ionization, i.e., two half-optical cycles later. For the 7 fs pulse, it is about 4 fs, or three half-optical cycles later. For the 14 fs pulse, it is two full optical cycles later. In other words, we can calibrate the kinetic energy peaks in Fig. 10 as reading of the molecular clocks at 2.6, 3.9 and 5.2 fs, reading from right to left. From the width of the peaks we can claim that the clock can be read with sub-femtosecond accuracy. Sequential double ionization of D_2 by short intense laser pulses has been studied by Legare *et al.*[12] but no pulse length dependence has been investigated experimentally yet.

also increases proportionally. Thus
nergy release will shift to the lower
energy distribution for an 8 fs pulse
gths. The single peak for each wave-
osition shifts to lower energy as the

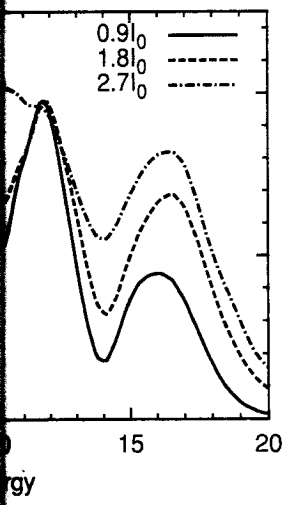

ral laser intensities with 30 fs pulse duration.
d return.

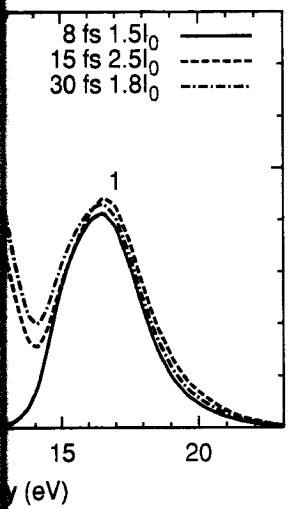

several laser intensities with different pulse
eturn peak.

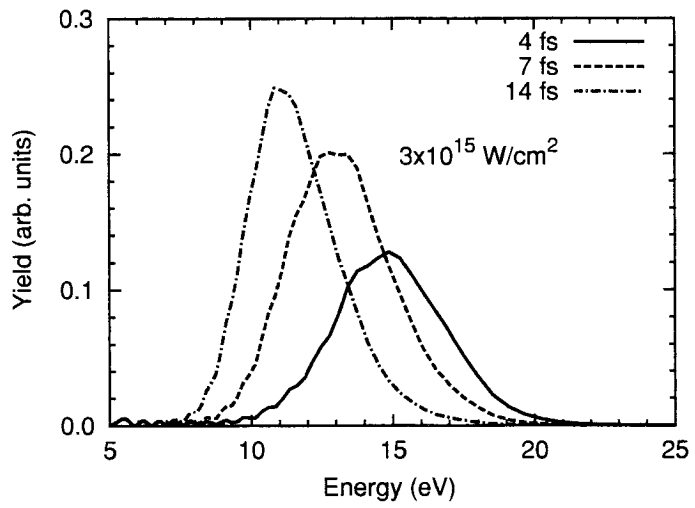

Fig. 10. Kinetic energy release spectra from sequential double ionization of D_2 for lasers with pulse durations of 4, 7, and 14 fs and peak laser intensity at 3×10^{15} W/cm^2.

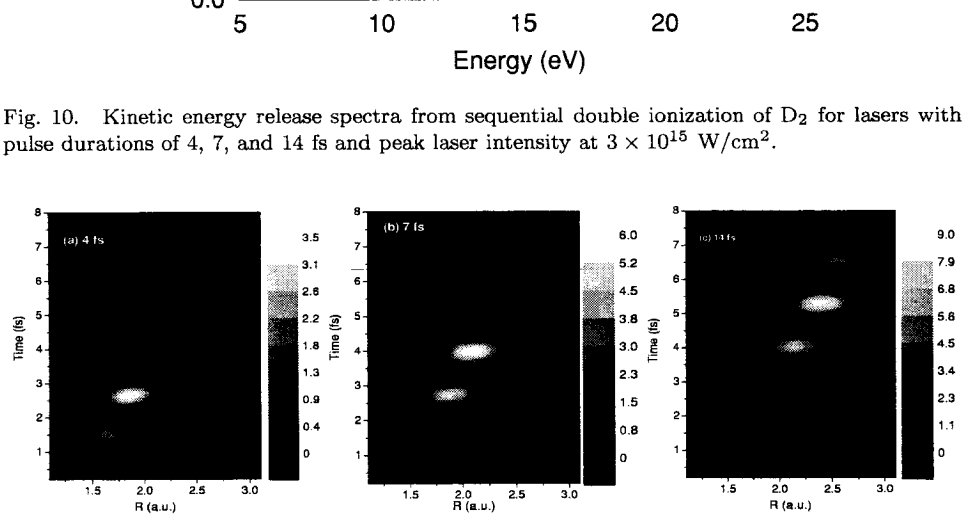

Fig. 11. 2D plot of sequential double ionization spectra versus time interval after the first ionization and the internuclear separation for lasers with pulse durations of 4, 7, and 14 fs and peak laser intensity at 3×10^{15} W/cm^2.

A molecular clock can be built based on short laser pulses in the intermediate intensity region, say about 4 I_0. In this case, both the rescattering and the sequential double ionization mechanisms can contribute to the double ionization and significant peaks can be identified from the kinetic energy release as well. Such experiment has been carried out.[14] In this case peaks in the kinetic energy release due to the rescattering and the sequential ionization can be identified and these peaks can be used to calibrate the molecular clock.

4. Summary and Conclusions

In this brief review we show how one can use the double ionization of D_2 molecules by short intense laser pulses to read clocks at sub-femtosecond accuracy based on

the kinetic energy release of t
iments where two laser pulse
employed here. The units of
of mean wavelength at 800
because the "pump" or first
depends sensitively on the in
ionization, due to either sequ
curs at sub-femtosecond accu
is not uniquely defined with
the first ionization occurs. T
physical processes leading to
We addressed all the element
the dominant mechanism at
of how a good understanding
in order to have a full grasp
interplay between the experi
of the double ionization of D_2
also witnessed the contributio
simplifying experimental kine
easier to handle.

Acknowledgments

This work was supported in pa
Division, Office of Basic Ene
Energy.

References

1. A. H. Zewail, *J. Phys. Che*
2. H. Niikura *et al.*, *Nature* **41**
3. H. Niikura *et al.*, *Nature* **42**
4. A. S. Alnaser *et al.*, *Phys.*
5. K. Codling, L. J. Frasinski
6. T. Seideman, M. Y. Ivanov
7. T. Zuo and A. D. Bandraul
8. E. Constant, H. Stapelfeldt
9. A. Giusti-Suzor *et al.*, *J. P*
10. K. Codling and L. J. Frasin
11. A. Bandrauk, *Comments A*
12. F. Legare *et al.*, *Phys. Rev.*
13. T. Osipov *et al.*, *J. Mod. O*
14. A. S. Alnaser *et al.*, *Phys.*
15. X. M. Tong and C. D. Lin,
16. B. M. Smirnov and M. I. C
JETP **22**, 585 (1966)].

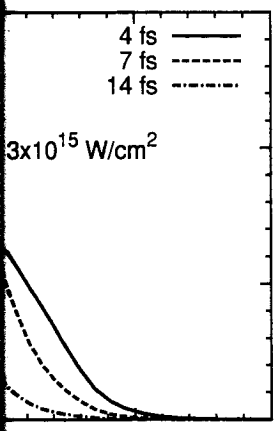

tial double ionization of D_2 for lasers with sity at 3×10^{15} W/cm^2.

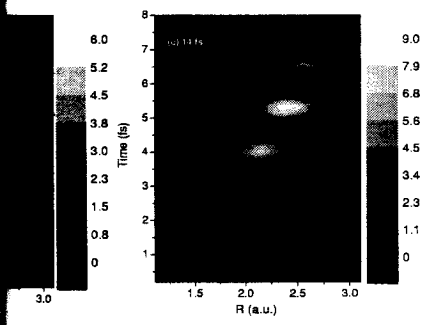

ctra versus time interval after the first ion- pulse durations of 4, 7, and 14 fs and peak

short laser pulses in the intermedi- case, both the rescattering and the contribute to the double ionization he kinetic energy release as well. Such se peaks in the kinetic energy release onization can be identified and these clock.

the double ionization of D_2 molecules t sub-femtosecond accuracy based on

the kinetic energy release of the D^+ ions. Unlike the standard pump–probe experiments where two laser pulses are needed, only a single femtosecond laser pulse is employed here. The units of time is the optical cycle which is 2.6 fs for a laser of mean wavelength at 800 nm. The sub-femtosecond accuracy can be achieved because the "pump" or first ionization is initiated by tunnelling ionization which depends sensitively on the instantaneous electric field. The "probe" is the second ionization, due to either sequential ionization or the rescattering process, also occurs at sub-femtosecond accuracy. While the starting time of the first ionization is not uniquely defined with respect to the laser pulse, the clock starts only after the first ionization occurs. To be able to read the clock, on the other hand, the physical processes leading to double ionization have to be understood thoroughly. We addressed all the elementary processes for the rescattering mechanism which is the dominant mechanism at lower intensity in details. It is a clear demonstration of how a good understanding of elementary atomic and molecular physics is needed in order to have a full grasp of intense laser physics. We have also shown the close interplay between the experiments and theory in rendering the full understanding of the double ionization of D_2 (or H_2) molecules by a single femtosecond pulse. We also witnessed the contributions of the recently developed few-cycle laser pulses in simplifying experimental kinetic energy spectrum which make the theoretical study easier to handle.

Acknowledgments

This work was supported in part by Chemical Sciences, Geosciences and Biosciences Division, Office of Basic Energy Sciences, Office of Science, U. S. Department of Energy.

References

1. A. H. Zewail, *J. Phys. Chem.* **A104**, 5660 (2000).
2. H. Niikura *et al.*, *Nature* **417**, 917 (2002).
3. H. Niikura *et al.*, *Nature* **421**, 826 (2003).
4. A. S. Alnaser *et al.*, *Phys. Rev. Lett.* **91**, 163002 (2003).
5. K. Codling, L. J. Frasinski and P. A. Hatherly, *J. Phys.* **B22**, L321 (1989).
6. T. Seideman, M. Y. Ivanov and P. B. Corkum, *Phys. Rev. Lett.* **75**, 2819 (1995).
7. T. Zuo and A. D. Bandrauk, *Phys. Rev.* **A52**, R2511 (1995).
8. E. Constant, H. Stapelfeldt and P. B. Corkum, *Phys. Rev. Lett.* **76**, 4140 (1996).
9. A. Giusti-Suzor *et al.*, *J. Phys.* **B22**, 309 (1995).
10. K. Codling and L. J. Frasinski, *J. Phys.* **B26**, 783 (1993).
11. A. Bandrauk, *Comments At. Mol. Phys.* **D1**(3), 97 (1999).
12. F. Legare *et al.*, *Phys. Rev. Lett.* **91**, 093002 (2003).
13. T. Osipov *et al.*, *J. Mod. Opt.* (in press) (2004).
14. A. S. Alnaser *et al.*, *Phys. Rev. Lett.* (in press) (2004).
15. X. M. Tong and C. D. Lin, *Phys. Rev. A* (accepted) (2004).
16. B. M. Smirnov and M. I. Chibisov, *Zh. Eksp. Teor. Fiz.* **49**, 841 (1966); [*Sov. Phys. JETP* **22**, 585 (1966)].

17. A. M. Perelomov, V. S. Popov and M. V. Terentev, *Zh. Eksp. Teor. Fiz.* **50**, 1393 (1966); [*Sov. Phys. JETP* **23**, 924 (1966)].
18. M. V. Ammosov, N. B. Delone and V. P. Krainov, *Zh. Eksp. Teor. Fiz.* **91**, 2008 (1986); [*Sov. Phys. JETP* **64**, 1191 (1986)].
19. A. Talebpour, C. Y. Chien and S. L. Chin, *J. Phys.* **B29**, L677 (1996).
20. A. Talbpour, S. Larochelle and S. L. Chin, *J. Phys.* **B31**, L49 (1998).
21. D. S. Guo, R. R. Freeman and Y. S. Wu, *Phys. Rev.* **A58**, 521 (1998).
22. M. J. DeWitt, E. Wells and R. R. Jones, *Phys. Rev. Lett.* **87**, 153001 (2001).
23. E. Wells, M. J. DeWitt and R. R. Jones, *Phys. Rev.* **A66**, 013409 (2002).
24. E. P. Benis *et al.*, *Phys. Rev. A* (accepted) (2004).
25. X. M. Tong, Z. X. Zhao and C. D. Lin, *Phys. Rev.* **A66**, 033402 (2002).
26. B. Shan *et al.*, *Phys. Rev.* **A66**, 061401 (2002).
27. Z. X. Zhao, X. M. Tong and C. D. Lin, *Phys. Rev.* **A67**, 043404 (2003).
28. I. V. Litvinyuk *et al.*, *Phys. Rev. Lett.* **90**, 233003 (2003).
29. A. S. Alnaser *et al.*, *Phys. Rev. Lett.* (in press) (2004).
30. X. Urbain *et al.*, *Phys. Rev.* **A92**, 163004 (2004).
31. P. B. Corkum, *Phys. Rev. Lett.* **71**, 1994 (1993).
32. G. L. Yudin and M. Y. Ivanov, *Phys. Rev.* **A63**, 033404 (2001).
33. G. L. Yudin and M. Y. Ivanov, *Phys. Rev.* **A64**, 035401 (2001).
34. I. Bray, CCC-database, http://atom.murdoch.edu.au/CCC-WWW/index.html.
35. Y. K. Kim, K. K. Irikura and M. A. Ali, *J. Res. NIST* **105**, 285 (2000).
36. J. M. Peek, *Phys. Rev.* **134**, A877 (1964).
37. X. M. Tong, Z. X. Zhao and C. D. Lin, *Phys. Rev.* **A68**, 043412 (2003).
38. X. M. Tong, Z. X. Zhao and C. D. Lin, *Phys. Rev. Lett.* **91**, 233203 (2003).
39. A. Staudte *et al.*, *Phys. Rev.* **A65**, 020703(R) (2002).
40. V. R. Bhardwaj *et al.*, *Phys. Rev. Lett.* **86**, 3522 (2001).

International Journal of Modern P
Vol. 18, No. 12 (2004) 1679–1685

TRIGGERED
C

Department of Physics,

The triggered stop-and-go tra
proach. The detailed phase
congestion is analyzed. The s
mechanism to trigger subsequ

Keywords: Traffic dynamics; t

1. Introduction

Highway traffic near the on-
Basically the traffic breakdow
of a one-dimensional non-equ
boundary effect to induce the
states can be categorized by
as a soliton-like stable struct
more complicate patterns ar
been identified.[2] Some are co
propagate quite far away fron
Among them, only one traffi
the triggered stop-and-go (T
supports the highest flow in t
come to the focus when one
large upstream flux.

The TSG state is charact
which triggers a new cluster a
a wide moving jam propagati
on-ramp has only negligible e
the ramp, the induced small
if the TSG state is activated,
the location of the on-ramp.

Full text articles are available at OCLC FirstSearch®.

Subscriptions, changes of address, single-copy orders should be addressed to Journal Department, World Scientific Publishing Co. Pte. Ltd., 5 Toh Tuck Link, Singapore 596224 or Suite 202, 1060 Main St., River Edge, NJ 07661, USA or 57 Shelton Street, Covent Garden, London WC2H 9HE, UK. Back issues are available.

The International Journal of Modern Physics B (ISSN 0217-9792) is published 3 times a month except for February, May, August and November (semi-monthly) (total 32 issues) by World Scientific Publishing Co. Pte. Ltd., 5 Toh Tuck Link, Singapore 596224. Subscription rates available upon request. Periodicals postage paid at JAMAICA, NY 11431.
US POST MASTER: Please send change of address to ***International Journal of Modern Physics B*** c/o Publications Expediting Services, 200 Meacham Avenue, Elmont, NY 11003. Air freight & mailing in the US by Publications Expediting Services, 200 Meacham Avenue, Elmont, NY 11003 (Tel. 516-352-7300). Printed in Singapore.

INTERNATIONAL

Vol.

Review Paper

Research Papers